Journal of Photochemistry & Photobiology, A: Chemistry 437 (2023) 114432

Contents lists available at ScienceDirect

Journal of Photochemistry & Photobiology, A: Chemistry

journal homepage: www.elsevier.com/locate/jphotochem

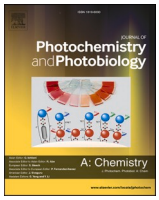

Molecular crowders modulate ligand binding affinity to G-quadruplex DNA by decelerating ligand association

Ndege Simisi Clovis [1], Parvez Alam [1], Ajay Kumar Chand, Deepika Sardana, Mohammad Firoz Khan, Sobhan Sen [*]

Spectroscopy Laboratory, School of Physical Sciences, Jawaharlal Nehru University, New Delhi 110067, India

ARTICLE INFO

Keywords:
G-quadruplex DNA
Ligand binding kinetics
Molecular crowder
Fluorescence correlation spectroscopy

ABSTRACT

The study of *kinetics* of ligand binding to G-quadruplex DNA (GqDNA) structures is of paramount importance for comprehending (possible) ligand-induced anticancer activity involving GqDNA within cells. However, cellular environment is *crowded* with variety of small- and macro-molecules that occupy ~30–40 % of cell-volume. While only few earlier studies dealt with deciphering the kinetics of ligands' interactions with GqDNA in dilute solution, such studies in cell-like crowded milieu are absent. Here we investigate the effect of small and macro molecular crowders, glucose, sucrose and ficoll 70, on the kinetic steps of association and dissociation of a benzophenoxazine-ligand (Cresyl Violet: CV) with human telometic (hybrid) GqDNA structure using fluorescence correlation spectroscopy (FCS), aided by other methods. We find that the binding constants of the ligand to GqDNA change appreciably with nearly fivefold decrease in the presence of ficoll 70, compared to that in pure buffer solution. FCS measurements unfold that this decrease of binding constants is mainly modulated by the viscosity-induced deceleration of the association of the ligand to GqDNA in the crowded solution; however, the rate-determining dissociation rates remain nearly unchanged in the presence of all three crowders. These results have important implications in the context of ligand/GqDNA interactions within cellular environment, which indicate that even if the binding affinity of a ligand to GqDNA structures may be influenced by cellular crowders, they may not influence the unbinding rate of the ligand from a stable ligand/GqDNA complex formed by strong π-π stacking interactions.

1. Introduction

The human telomeric DNA contains tandem repeats of $d(TTAGGG)_n$ sequence which can form G-quadruplex structures with various folding topologies in the presence of cations [1–4]. These polymorphic G-quadruplex DNA (GqDNA) structures are also found to form in promoter regions of different oncogenes [4]. These GqDNA structures play vital role in various biochemical processes inside cells, including protection of chromosome ends [5,6], expression of genes [7,8], and transcription [9,10]. More importantly, the GqDNA structures have been found to be promising target sites for small molecular ligands which often show anticancer activity [11–17]. In effect, the study of interactions of small molecular ligands with GqDNA and ligand-induced stability of such GqDNA structures, leading to (possible) anticancer activity, remains in the forefront of active research. Such activity led to the development of numerous quadruplex-specific small molecular ligands [11–18]. However, most of previous studies on ligand/GqDNA interaction stressed on determining the ligand binding affinity and thermodynamics of ligand binding as well as ligand-induced stabilization of GqDNA, but information on the *kinetics* of such interaction remains limited. Thus, it has been difficult to comprehend how binding *kinetics* (association and dissociation rates) of ligands with GqDNA control their binding affinities, and also, how environmental conditions affect such kinetics?

While only a few kinetic studies on ligand/GqDNA interactions unfolded the role of association and dissociation rates on defining the overall ligand binding affinity to GqDNA structures and also found the rate determining step(s) of such interactions in dilute solution [19–21], it is still unknown how molecular crowders affect such kinetic rates to control the overall binding affinity of ligands to GqDNA. In reality, the cellular environment where most of the fundamental biochemical reactions occur, including ligand/GqDNA interactions, is extremely crowded with small and macromolecular entities. The total

* Corresponding author.
E-mail address: sens@mail.jnu.ac.in (S. Sen).
[1] Authors contributed equally.

https://doi.org/10.1016/j.jphotochem.2022.114432
Received 29 September 2022; Received in revised form 30 October 2022; Accepted 18 November 2022
Available online 21 November 2022

concentration of many of such soluble and insoluble (macro) molecules within cells can be very high [22–25]: For example, the concentrations can vary from one cell to another like, ~50–400 mg/ml in Eukaryotic cells, ~300–400 mg/ml in Escherichia coli, nearly 80 mg/ml of solutes in blood plasma, ~270–560 mg/ml in mitochondria, and approximately 400 mg/ml in nucleus. However, it is challenging to study the structure, dynamics and molecular interactions of biomolecules (proteins and nucleic acids) within such crowded cellular environment directly. Thus, researchers often adopt a satisfactory route to mimic cell-like environment in the *in vitro* experimental conditions by adding large amounts of background co-solutes/co-solvents in the solution, known as molecular crowders, and study the properties of molecules-of-interest within such crowded solution [26–41].

It is well-established from *in vitro* studies in crowded condition that structure, dynamics and interactions of biomolecules get substantially perturbed, compared to that in dilute condition, which are often explained by invoking the effects of crowding induced excluded volume as well as changes in viscosity, specific or non-specific interactions, water activity, osmotic stress, and environmental dielectric constant [26–41]. Several earlier reports showed that crowders have stabilizing effects on biomolecules such as proteins, enzymes and their activity [31–34], and on nucleic acid structures [26–28]. More so, in a study involving small peptides, Gai and co-workers showed that common molecular crowders, such as PEG, dextran, ficoll do not affect the folding of peptides to a great extent, but the helix-to-coil transition shows viscosity dependence [35]. Weiss and co-workers reported single molecule study to show that molecular crowding enhances the rate of initiation and promoter clearance in enzymatic reaction involving RNA polymerase, and observed that this enhancement of rate was dependent on the molecular crowders' size [36]. Kovermann and co-workers studied crowding effect on interaction of single-stranded DNA with cold shock protein B (CspB) to show that EG, PEG, glucose and dextran decelerate association of DNA and protein substantially, although, the dissociation rates are critically controlled by the chemical properties of crowders [37]. The insufficiency of only excluded volume effect was also envisaged in a computational study by Dey and Bhattacharjee on DNA-protein interactions in the presence of high concentration of molecular crowders [38]. This study showed molecular crowders create depletion (hydration) layer of ~7–13 Å between the DNA-backbone and crowder molecules, which is crowder concentration dependent. The crowders although, enhances overall macro-viscosity of solution, the depletion (hydration) layer maintains a constant (micro) viscosity to facilitate DNA target search of the protein [38]. A more recent single molecule FRET (smFRET) study by Schuler and co-workers showed that a series of PEG crowders accelerate the association rates of two intrinsically disordered proteins (IDPs) through depletion-induced interaction at low crowder concentration, but decelerate the association rate through viscosity-induced interaction at higher crowder concentrations [39]. These observations indicate that excluded volume effect is not the only mechanism to explain the complete effect of molecular crowders on biomolecular interaction kinetics. Nevertheless, it is still unknown how molecular crowders affect ligand binding kinetics with GqDNA.

Synthetic crowding agents, such as different molecular weight PEGs (and its monomer), saccharides, organic solvents, osmolytes, etc. have been used to study their effect on stabilizing GqDNA structures [26–28]. It was envisaged that crowding induced change in local hydration/solvation can induce folding of GqDNA structures [27,28], which also affect binding affinities of ligands to GqDNA significantly [29,30,41]. However, these earlier studies focused on the structural polymorphism and stability of GqDNA, and the thermodynamics of ligand binding to various GqDNA structures in crowded milieu. Instead, probing and understanding the kinetic steps of ligand binding/unbinding with GqDNA remained sparse, and that too only in dilute solution [19–21,42]. Although knowledge of thermodynamics of these process is crucial to identify the stable (bound and unbound) states and the binding free energy, the kinetics of such interactions provide mechanistic insight of the rate-determining step(s) which control the binding affinity of a ligand to a biomolecule in an intricate way. Thus, the questions remain – how molecular crowding affects ligand binding kinetics with GqDNA? And also, what is (are) the rate determining step(s) of such reaction kinetics and whether they are crowder dependent?

In this paper, we tackle these questions through comprehensive fluorescence correlation spectroscopic (FCS) studies at (near) single molecule level on the binding kinetics of a benzophenoxazine-ligand (cresyl violet: CV) with (3 + 1) hybrid GqDNA structure formed by human telomeric sequence in the absence and presence of 20 % (w/v, i.e., 200 mg/ml) saccharide crowders, viz., glucose, sucrose and ficoll 70. The concentration (20 % w/v) used here is comparable to the cellular crowder concentrations, and also that all these three sugars have similar volume exclusion in solution [43,44]. The choice of crowders were also made based on previous studies which showed that ficoll 70 and Xenopus laevis egg extract are rather inert crowders which only marginally affect modulating GqDNA structure of telomeric DNA sequences [37,40]; however, commonly used PEG can drastically affect the GqDNA topology [26,28,38,41]. Here we include the monomer and dimer of the saccharides to also probe the crowder-size dependence on the rates of ligand binding kinetics with GqDNA at similar volume exclusion of the crowders in solution.

The ligand/GqDNA interaction proceeds on a complex free-energy landscape where the freely diffusing ligand and GqDNA interact with each-other to form an (intermediate) encounter complex controlled by (diffusive) forward and backward rate constants (k_d and k_{-d}). Out of many such encounter complexes only few get fused to form the stable ligand/GqDNA complex, which is controlled by the other two rate constants (k_r and k_{-r}) (see Fig. 1). Using FCS we measure the rate constants by correlating the fluorescence fluctuations of the ligand (CV) which arise from the high and low fluorescence states of the ligand in its free and bound states, followed by fitting the correlation curves altogether with suitable model function and subsequent calculations. We show that the measured binding constants of the ligand to GqDNA in absence and presence of the crowders change appreciably, where the binding constant decreases by more than twofold in the presence of smaller crowders (glucose and sucrose) and fivefold in the presence of larger ficoll 70 crowder, compared to that in the absence of crowders. The measured kinetic rate constants from FCS show that the decrease in binding constant of ligand to GqDNA is modulated by the viscosity-induced deceleration of the overall association (k_+), which is mainly controlled by the change in (diffusive) forward and backward rate constants (k_d and k_{-d}), forming the encounter complex, and the association rate (k_r) of the encounter complex to make the stable complex. Surprisingly however, we observe that the ligand dissociation rates (k_{-r}) from its DNA-bound state (the rate-determining step) are nearly unaffected by the crowders. These results suggest that the chemical nature and/or size of the crowders do not influence the stable π-stacking interaction of the ligand with the G-tetrad within GqDNA. These observations indicate that even though the binding affinity of a ligand to GqDNA may be influenced by cellular crowders through viscosity-induced deceleration of association of reactants, the stable ligand binding to G-tetrad through π-π stacking may remain nearly unaffected by the crowders, giving rise to similar activation energy barriers for ligand unbinding from the GqDNA in the absence and presence of crowders.

2. Results and discussion

2.1. Circular dichroism data show marginal effect of crowders on structure and stability of GqDNA and Ligand/GqDNA complex

We confirm the formation of (3 + 1) hybrid GqDNA structure from CD measurement. The CD spectra of (3 + 1) hybrid GqDNA in absence and presence of the crowders are shown in Fig. 2A. Characteristic peaks of higher order GqDNA hybrid structure are observed; a large positive

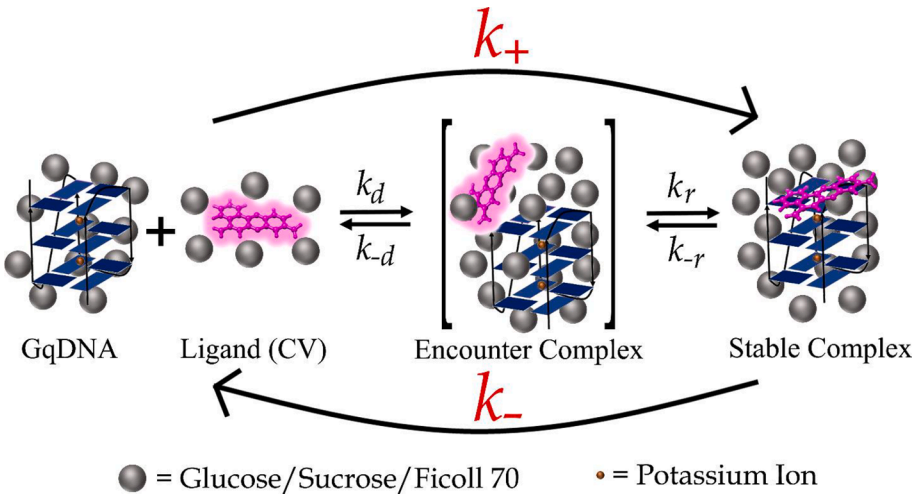

Fig. 1. Schematic showing ligand (CV)/GqDNA interaction kinetics in the presence of molecular crowders. The ligand/GqDNA complex formation occurs through a complex free-energy landscape where the reactants (ligand and GqDNA) diffuse freely to interact with each-other to form an (intermediate) encounter complex where the ligand comes within the solvation shell of GqDNA, followed by tight binding of the ligand with G-tetrad of GqDNA through π-π stacking interaction. All the rate constants for these processes are depicted in the scheme.

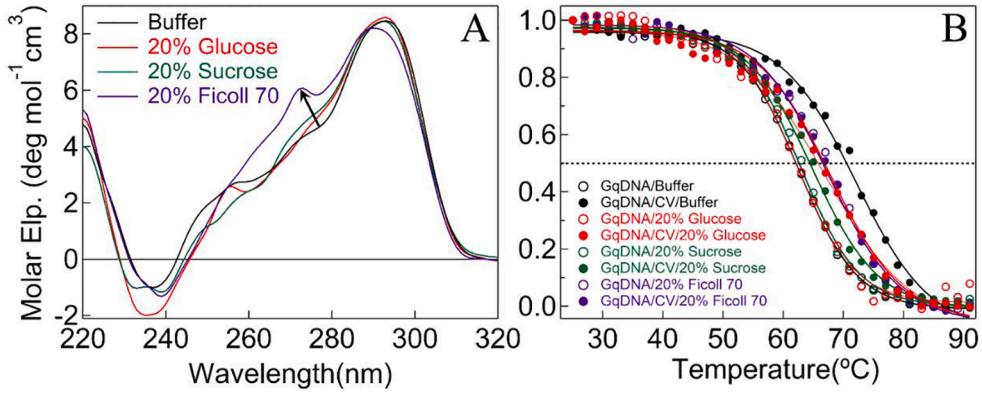

Fig. 2. (A) CD spectra of GqDNA formed by 22-mer human telomeric sequence in the presence of K^+ ions of those formed in the absence and presence of 20 % (w/v) glucose, sucrose and ficoll 70. Data show typical signature of formation of (3 + 1) hybrid GqDNA structure. It is observed that glucose and sucrose do not affect the hybrid GqDNA structure, while the ficoll 70 produce subtle effect on the structure. (B) Melting curves of (3 + 1) hybrid GqDNA structure measured at 290 nm of CD curves in the absence and presence of ligand and the molecular crowders (see legends for systems): buffer (black), glucose (red), sucrose (green) and ficoll 70 (purple). The lines through points are the sigmoidal fits to the melting data. The melting temperature (T_m) obtained from the 50 % change of the CD (see Table 1). (For interpretation of the references to colour in this figure legend, the reader is referred to the web version of this article.)

peak at ~290 nm, a positive shoulder at ~275 nm, a small hump at ~255 nm and a negative peak at ~238 nm signify the formation of hybrid GqDNA structure, similar as observed earlier [20,28]. Importantly, we observe that both glucose and sucrose do not affect the overall topology of the GqDNA, while ficoll 70 marginally modulate the structure (Fig. 2A), similar as observed previously [37,40]. The increase in CD signal of the hump near 275 nm in case of ficoll 70 indicate a small effect of the crowder to induce the structure little toward parallel GqDNA conformation. However, this increase in the positive signal is small enough that the overall GqDNA structure remains (3 + 1) hybrid type. A very similar feature was also observed earlier for hybrid GqDNA formed by other DNA sequences in the presence of ficoll 70 [37,40]. These data suggest that the branched poly-saccharide crowder of higher molecular weight has only subtle effect on the GqDNA structure, but other smaller crowders do not affect the GqDNA structure at physiological crowder concentration. This situation may also hold within cells because similar effect on GqDNA structure was observed earlier when Xenopus laevis egg extract was used as background molecular crowder [40].

We also observe that the smaller crowders do not change the melting temperature (T_m) of GqDNA, suggesting insignificant impact of the smaller crowders on the stability of GqDNA structure, though a stabilizing effect is observed for ficoll 70 which increases the T_m by ~5 °C compared to that in only buffer (Fig. 2B and Table 1). This is in line with the subtle impact of ficoll 70 on the topology of GqDNA. These effects may arise from the subtle change in the local dielectric environment and/or water activity within the solvation shells around GqDNA, induced by the crowder [23,26]. Importantly, the ligand binding to GqDNA increases the melting temperature (T_m) nearly by 10 °C compared to that in the absence of ligand in pure buffer (Table 1), which represents an enhancement in the stability of the structure. However, all crowders decrease the stability of the ligand/GqDNA complex by decreasing the T_m by almost similar extent. These results indicate that the crowders may decrease the ligand binding affinity to induce destabilization of the ligand/GqDNA complex. These observations are in line with previous report that showed similar crowding effects by PEG 200 on GqDNA stability in the presence of other ligands (TMPyP4, BMVC

Table 1
Melting temperatures (T_m) of (3 + 1) hybrid GqDNA structure in different solution conditions measured from temperature-dependent CD data at 290 nm.

Systems	T_m (°C)
GqDNA in Buffer	62.6 (±0.2)
GqDNA in 20 % Glucose	62.1 (±0.4)
GqDNA in 20 % Sucrose	62.9 (±0.2)
GqDNA in 20 % Ficoll 70	67.4 (±0.3)
CV/GqDNA in Buffer	72.1 (±0.4)
CV/GqDNA in 20 % Glucose	67.2 (±0.5)
CV/GqDNA in 20 % Sucrose	64.8 (±0.2)
CV/GqDNA in 20 % Ficoll 70	67.9 (±0.3)

and Hoechst) [30].

2.2. Molecular crowding decreases binding affinity of ligand to GqDNA

Investigations on the effect of molecular crowders on the ligand binding to GqDNA have shown drastic effect on ligand/GqDNA stabilization as well as binding constant of ligands [29,30,41]. Notably, interaction of ligands having benzophenoxazine core-group with GqDNA structures have been studied [17,20], and it has been shown that benzophenoxazine-ligands can down-regulate the c-KIT expression through interaction with GqDNA in gastric cancer cells [17]. However, it is unknown how cellular crowding affect the ligand's interaction with GqDNA.

Here we use a common benzophenoxazine ligand, cresyl violet (CV) which show strong fluorescence when free in solution; however, when it binds through π-stacking to the G-tetrad of GqDNA its fluorescence quenches due to strong electron transfer from the guanines to the ligand. Fig. 3 shows the relative fluorescence intensity decrease of CV upon binding to GqDNA in absence and presence of 20 % (w/v) glucose, sucrose and ficoll 70. In all cases the fluorescence intensity of CV (10 nM) in buffer with peak at ~626 nm is drastically quenched and slightly red-shifted with increase in GqDNA concentration (0 to 50 μM). However, the maximum extents of quenching in the absence and presence of crowders are slightly varied within the same concentration range of GqDNA, possibly due to local environmental/solvation effect induced by the crowders which influence the efficiency of electron transfer from guanines to CV. It is important to note here that we have measured the control spectra of CV only in the presence of the crowders (without GqDNA) to see if the fluorescence quenching is primarily due to binding of the ligand to G-tetrad or not. We observe that in the absence of GqDNA the fluorescence signal of CV increases by ~2.5 fold in the presence of all three crowders, instead of quenching, possibly due to change in environmental dielectric constant and/or viscosity (data not shown). This proves that the observed quenching of CV fluorescence is exclusively due to its binding to the G-tetrad and subsequent electron transfer from guanines to the ligand.

Fig. 3E plots the relative fluorescence quenching of CV with GqDNA concentration, along with the fits using equation S1 (supplementary material) to obtain the binding constants (K) of CV to GqDNA in absence and presence of crowders. Table 2 and Fig. 3F include the measured binding constants and bar-graph, respectively. We observe that the binding constants decrease by nearly-two fold in the presence of glucose and sucrose, but more than fivefold in the presence of ficoll 70. This is in line with the decrease of melting temperature of ligand/GqDNA complex in the presence of crowders. Similar, but more drastic effect of co-solvent crowding on ligand binding to GqDNA was also observed earlier [41]. Nevertheless, it is difficult to understand how the molecular crowders affect the binding kinetics (association and dissociation) to control the overall binding constants of the ligand to GqDNA.

2.3. Fluorescence correlation spectroscopy (FCS) data

2.3.1. FCS data unravel important kinetic parameters of ligand/GqDNA interactions

One needs techniques with high time-resolution and broad dynamic time-range to measure the reaction rates of ligand binding/unbinding with a target biomolecule, especially with GqDNA [19–21]. In fact, it has been found that Surface Plasmon Resonance (SPR), a widely used technique for measuring association and dissociation rates of ligands with biomolecules, cannot provide accurate rate constants of ligand/GqDNA interactions due to its limited time-resolution [19,42,45]. However, FCS is ideal for measuring such reaction rates of ligand/biomolecule interactions as it can probe molecular processes from picoseconds to seconds with single molecule sensitivity. FCS measures

Table 2
Binding constants of CV with (3 + 1) hybrid GqDNA structure obtained from data in Fig. 3E at different solution conditions.

Systems	Binding Constant K ($\times 10^6$ M^{-1})
CV/GqDNA in Buffer	3.12 (±0.15)
CV/GqDNA in 20 % Glucose	1.85 (±0.03)
CV/GqDNA in 20 % Sucrose	1.38 (±0.07)
CV/GqDNA in 20 % Ficoll 70	0.58 (±0.01)

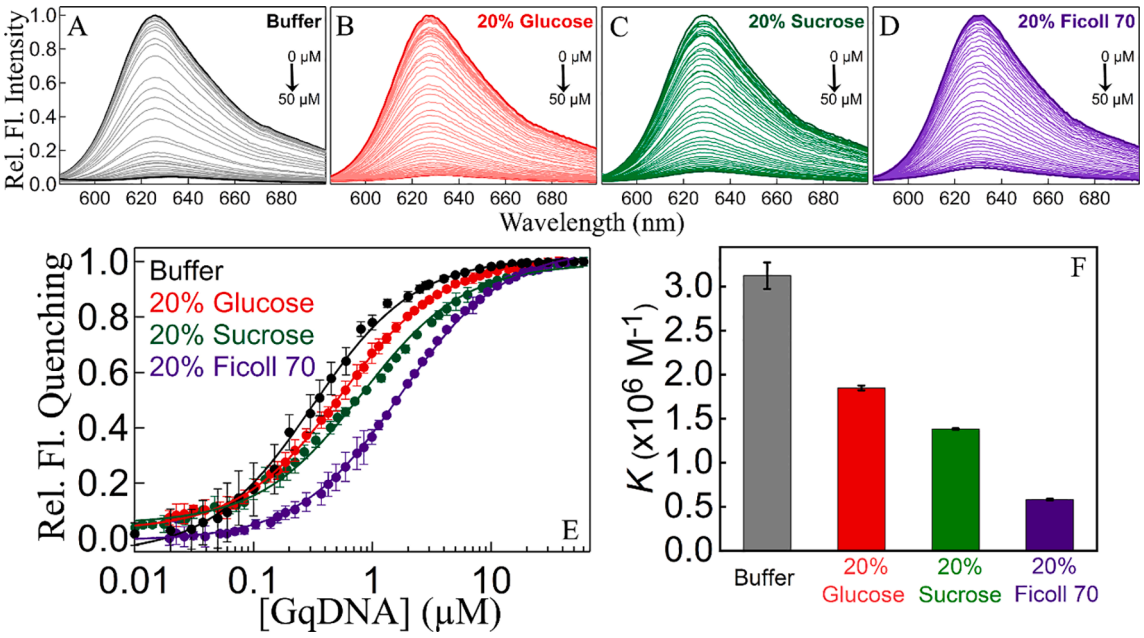

Fig. 3. Relative quenching of fluorescence spectra of cresyl violet (CV) with increasing GqDNA concentrations in (A) buffer, (B) 20% (w/v) glucose, (C) 20% (w/v) sucrose and (D) 20% (w/v) ficoll 70. (E) The relative fluorescence quenching with GqDNA concentration, along with fits using equation S1. (F) Bar-graphs plotting the measured binding constants of CV to GqDNA from the fits to data in (E) in the absence and presence of the crowders. Error bars are obtained from triplicate measurements. (For interpretation of the references to colour in this figure legend, the reader is referred to the web version of this article.)

processes occurring at different time-scales by correlating fluorescence fluctuations that arise from spontaneous changes of molecular concentration and/or the fluorescence states of a reporter probe due to chemical reaction during probe's free diffusion in-and-out of a tiny observation volume created by a laser light within solution in a confocal configuration [46–48]. FCS was used to measure the association and dissociation rate constants of fluorescent [20,21] and non-fluorescent [19] ligands with GqDNA, and also ligand-induced folding of GqDNA structures [49]. Furthermore, FCS has been implemented successfully to observe the charge-transfer dynamics in DNA [50], i-motif folding [51], base-mismatch dynamics [52], protein conformational fluctuations [33,34,53–57], amyloid aggregation [58,59], Ras-dynamics in fungal-membrane [60], cyclodextrin/ligand interaction [61] as well as to measure the accurate size-parameters of microemulsion droplets [62,63] and their interactions for synthesizing nano-materials [64], to mention a few.

Here we perform FCS measurements using a modified FCS-setup with under-filled objective back-aperture for excitation laser (larger confocal volume) – so as to make the reaction and diffusion of ligand/GqDNA system separated in time, similar as implanted by us earlier [19,20]. Fig. 4 shows the measured fluorescence correlation curves of ligand (CV, 1 nM) with varying GqDNA concentrations (0 to 30 μM) in the absence and presence of 20 % (w/v) crowders. The FCS data show reaction-coupled diffusive correlation curves where the ligand/GqDNA interaction (reaction) occurs below ~600 μs and the diffusion occurs above this time-range. It is clearly observed that as we increase GqDNA concentration the reaction-time gets faster and the reaction-amplitude first increases and then decreases in a concentration dependent manner. On the other hand, diffusive correlation part gets slower monotonically with the increase in GqDNA concentration, indicating more and more ligand/GqDNA complex formation within the solution. These trends of FCS data remain similar in the presence of crowders, except for small modulations in reaction-amplitude but drastic change in diffusion of the complex due to solution viscosity increase.

Considering the interaction of ligand (CV) and GqDNA as a single-step bimolecular reaction with k_+ and k_- as association and dissociation rate constants, respectively, one can write the following,

$$CV + GqDNA \underset{k_-}{\overset{k_+}{\rightleftharpoons}} CV - GqDNA \tag{1}$$

Here, the equilibrium binding constant (K) can be expressed as,

$$K = \frac{k_+}{k_-} \tag{2}$$

Within above description, the correlation curves can be modelled in a global target fit using following equation which incorporates the reaction term and the average number of free and bound ligands, and their diffusion inside the observation volume [19,20,61].

$$G(\tau) = \frac{1}{N_f + N_b}\left(1 + \left(\frac{\tau}{\bar{\tau}_D}\right)\right)^{-1}\left[1 + s\left(\frac{\tau}{\bar{\tau}_D}\right)\right]^{-1/2}\left[1 + A_R e^{-\frac{\tau}{\tau_R}}\right] \tag{3}$$

In this equation, N_f and N_b are the average number of free and bound ligands inside the observation volume, respectively, $\bar{\tau}_D$ is average diffusion time, s is instrument factor, A_R is reaction amplitude and τ_R is the reaction-time which can be expressed in terms of the rate constants as [19,20,61],

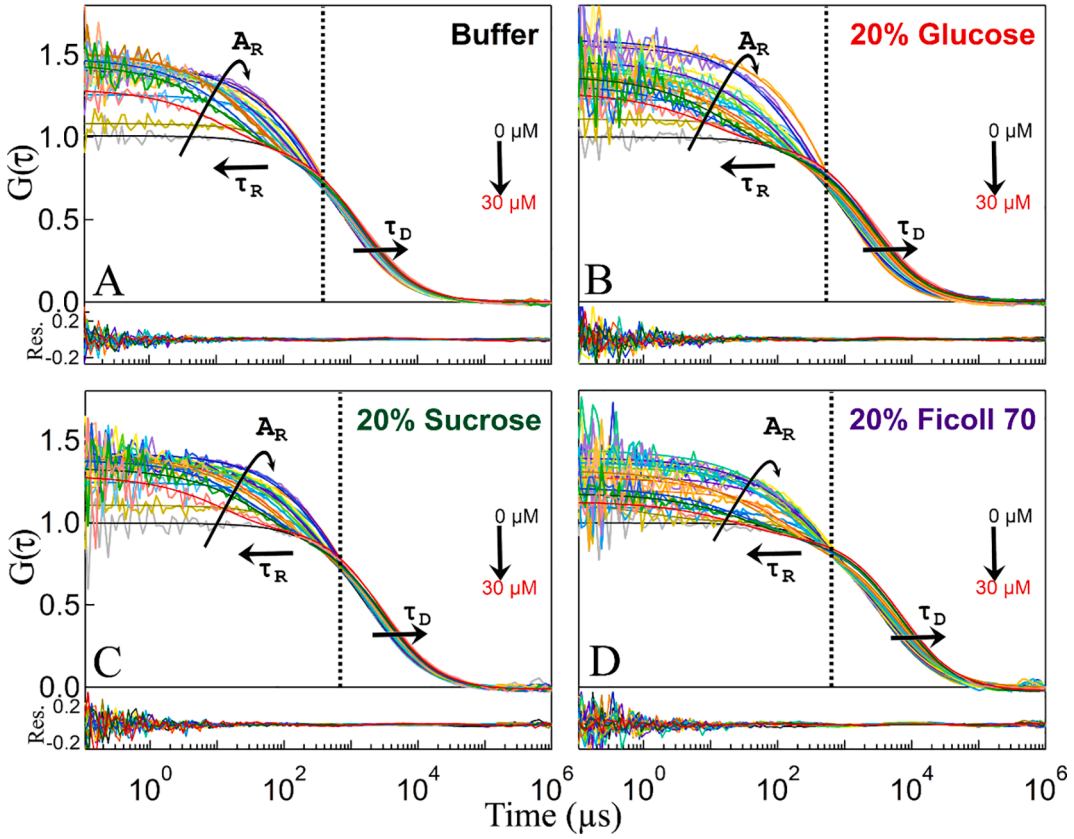

Fig. 4. Normalized fluorescence correlation curves of cresyl violet (CV) with varying concentrations of (3 + 1) hybrid GqDNA in (A) buffer, (B) 20 % w/v glucose, (C) 20 % w/v sucrose and (D) 20 % w/v ficoll 70. Plots also include the (global) fits to the data-sets using Eq. (5), along with the residuals-of-fits. The correlation data show typical characteristics of GqDNA concentration dependent change of reaction-time, reaction-amplitude and diffusion time. See Fig. S1 for the variation of reaction time and amplitude and Table 1 for the estimated kinetic parameters. (For interpretation of the references to colour in this figure legend, the reader is referred to the web version of this article.)

$$\tau_R = \frac{1}{k_+[GqDNA] + k_-} = \frac{1}{k_-(1 + K[GqDNA])} \quad (4)$$

Modelling of GqDNA-concentration dependent FCS data altogether using Eq. (3) in a global target fit was rather unsatisfactory, especially in the reaction part of the correlations; hence, we modified Eq. (3) by incorporating a stretch exponent (β) to the (exponential) reaction term as,

$$G(\tau) = \frac{1}{N_f + N_b}\left(1 + \left(\frac{\tau}{\overline{\tau}_D}\right)\right)^{-1}\left[1 + s\left(\frac{\tau}{\overline{\tau}_D}\right)\right]^{-1/2}\left[1 + A_R e^{-\left(\frac{\tau}{\tau_R}\right)^{\beta}}\right] \quad (5)$$

This situation can arise when there are overlapping relaxation kinetics, instead of a unique one, which is likely as the ligand can bind to the G-tetrad by π-stacking having different angle of orientations. Such angle-dependent multiple local minima of ligand binding to G-tetrad was observed in molecular dynamics simulation study of ligand (*berberine*) binding to parallel-GqDNA structure [65]. Similar stretched exponential-type relaxation was also observed for DNA hairpin folding/unfolding kinetics [66] and blinking photophysics of cyanine dyes [67].

Fig. 4 includes the fits and residuals obtained from global fit of full-dataset altogether using Eq. (5). In this global fit, s was a fixed global parameter, while β was a free global parameter and $\overline{\tau}_D$, A_R and τ_R were GqDNA-concentration dependent free parameters. Fig. S1 (in Supporting Material) compares the fits to correlation curves of CV in the presence of 5 μM GqDNA using Eqs. (3) and (5) in the absence and presence of the crowders. As can be seen, the residuals of the fits are much improved in the fits using Eq. (5) that incorporates a stretched exponent to the reaction-time considering overlapping relaxation kinetics of the ligand/GqDNA interactions. Similar improvements in residuals are also observed in the fits to other correlation curves using Eq. (5), measured at other GqDNA concentrations (data not shown). Following the fits using Eq. (5), the concentration dependent average reaction-time of the ligand/GqDNA interactions were obtained as [66,67],

$$\langle \tau_R \rangle = \left(\frac{\tau_R}{\beta}\right)\Gamma\left(\beta^{-1}\right) \quad (6)$$

Here $\Gamma(\beta^{-1})$ is the gamma function. For calculating the dissociation rate constants (k_-), the GqDNA-concentration dependent $\langle \tau_R \rangle$ variations are fitted using Eq. (4), where we fixed the values of binding constants (K) obtained from the steady-state measurements (Table 2) (see Fig. S2 for fits to τ_R vs. [GqDNA] plots). Finally, the association rate constants (k_+) are obtained from Eq. (2) using the above k_- and the K values (from steady-state measurements).

At this juncture, it is important to check if the reaction-coupled diffusive correlations are the manifestations of the ligand/GqDNA interactions and not the (non-specific) interactions of the ligand with crowders. As found in Fig. 4 (and also Fig. S3) the correlation curves of CV in the presence of crowders, but in absence of GqDNA, do not show any reaction-coupled correlation in the faster time-scale. Thus, the GqDNA-concentration dependent reaction-coupled diffusive correlations (Fig. 4) only originate from the ligand/GqDNA interactions.

Table 3 incorporates the association and dissociation rate constants obtained from the FCS data of CV/GqDNA interaction in the absence and presence of crowders. The most important observation in this data-set is that the decrease in binding constants of ligand to GqDNA in the presence of crowders is *mainly controlled by the deceleration of association* (k_+) of the ligand to GqDNA, which decrease by nearly fivefold on going from pure buffer to 20 % ficoll solution. On the other hand, the dissociation rate constants (k_-) remain nearly similar (within error limit) in all cases. These striking results are unique in the context of ligand/GqDNA interactions in crowded milieu that indicate – once the ligand finds its binding site within GqDNA through faster or slower association, the crowders do not modulate the π-stacking interaction of the ligand with G-tetrad, such that the activation barrier of ligand-unbinding remains nearly unaffected by the crowders, be it smaller or larger crowders, despite the fact that they do decrease the overall ligand binding affinity to GqDNA and the stability (T_m) of the ligand/GqDNA complex (see above).

2.3.2. *The viscosity-induced diffusive kinetic rate constants control the ligand binding affinity to GqDNA*

Though the above results showed overall association rate of ligand to GqDNA is the main factor that modulate the ligand's binding constants to GqDNA in the presence of crowders, it is still difficult to envisage why such association rate is the dominating factor. In order to ascertain further mechanistic details of the interaction, we consider the process to be occurring through free diffusion of the reactants (ligand and GqDNA) which first form an (intermediate) encounter complex where the ligand comes within the solvation-shell of GqDNA, followed by the π-stacking of the ligand with G-tetrad to make the stable complex (see Fig. 1). These processes are controlled by four rate constants as depicted in Fig. 1.

For freely diffusing ligand and biomolecule which encounter with each-other, the diffusion controlled (forward) collisional rate constant (k_d) can be calculated from the knowledge of diffusion constants and sizes (hydrodynamic radii) of the individual entities through Smoluchowski equation [68],

$$k_d = 4\pi\left(D_{CV} + D_{GqDNA}\right)\left(Rh_{CV} + Rh_{GqDNA}\right)N_{av} \quad (7)$$

Here, D_{CV} and D_{GqDNA} are the diffusion constants of the ligand and the GqDNA, respectively, while Rh_{CV} and Rh_{GqDNA} are the hydrodynamic radii of the ligand and GqDNA, respectively, and N_{av} is Avogadro number.

We measured the solution (micro) viscosity in the presence of crowders using Rhodamine-6G as tracer particle employing FCS measurements at single molecule level (with over-filled objective back-aperture of excitation laser, i.e., small diffraction-limited confocal volume). Using these viscosities, the sizes (hydrodynamic radii) and diffusion constants of CV and GqDNA (using a Cy3-labelled hybrid-GqDNA) in crowded solutions are measured independently at single molecule level using same FCS setup with over-filled objective back-aperture. The FCS data with fits are shown in Fig. S4 and the measured parameters are included in Table S1 (Supporting Material). These parameters (sizes and diffusion constants) are then used to calculate the diffusion controlled (forward) collisional rate constant, k_d using Smoluchowski equation (7). Table 3 includes the calculated

Table 3
Ligand binding and kinetic parameters estimated from steady-state fluorescence and FCS measurements for CV/GqDNA interactions.

System CV/GqDNA	K ($\times 10^6$ M^{-1})	k_+ ($\times 10^9$ $M^{-1}s^{-1}$)	k_- ($\times 10^3$ s^{-1})	k_d ($\times 10^9$ $M^{-1}s^{-1}$)	k_{-d} ($\times 10^9$ s^{-1})	K_{enc} (M^{-1})	k_r ($\times 10^9$ s^{-1})	k_{-r} ($\times 10^3$ s^{-1})	K_{reac} ($\times 10^5$)
In Buffer	3.12 (±0.15)	2.07 (±0.14)	0.66 (±0.03)	11.34 (±0.68)	1.03 (±0.08)	11.01 (±1.08)	0.23 (±0.03)	0.81 (±0.14)	2.84 (±0.31)
In 20 % Glucose	1.85 (±0.03)	1.36 (±0.06)	0.74 (±0.03)	5.46 (±0.67)	0.50 (±0.08)	10.92 (±2.20)	0.16 (±0.04)	0.95 (±0.30)	1.69 (±0.34)
In 20 % Sucrose	1.38 (±0.07)	0.91 (±0.04)	0.66 (±0.03)	5.48 (±0.63)	0.48 (±0.07)	11.42 (±2.12)	0.09 (±0.02)	0.74 (±0.21)	1.21 (±0.22)
In 20 % Ficoll 70	0.58 (±0.01)	0.46 (±0.06)	0.79 (±0.10)	1.67 (±0.18)	0.28 (±0.04)	5.96 (±1.07)	0.10 (±0.02)	1.03 (±0.27)	0.97 (±0.17)

collisional rate constant, k_d for all systems studied.

The encounter complex can again dissociate with a rate constant, k_{-d} which can be estimated from the time needed for the ligand and the biomolecule to diffuse apart by at least the total molecular sizes of the ligand and biomolecule (added sizes). Thus, the equilibrium constant of the encounter ($K_{enc} = k_d/k_{-d}$) can be expressed as the volume occupied by the ligand and GqDNA [61]. Hence one can write [61],

$$\frac{k_d}{k_{-d}} = \pi\left(Rh_{CV} + Rh_{GqDNA}\right)^3 N_{av} \Rightarrow k_{-d} = \frac{k_d}{\pi\left(Rh_{CV} + Rh_{GqDNA}\right)^3 N_{av}} \tag{8}$$

The values of k_{-d} are obtained from Eq. (8) using the k_d values and the sizes of the individual components obtained above (Table 3).

One can also define the equilibrium constant (K_{reac}) for the formation of the final stable complex from the intermediate encounter complex as,

$$K_{reac} = \frac{k_r}{k_{-r}} \tag{9}$$

The overall equilibrium binding constant can then be expressed as, $K = K_{enc} \times K_{reac}$. Assuming the unbinding rate (k_{-r}) of ligand from stable complex of π-stacked bound-state with G-tetrad is low enough, we obtain the forward rate constant of the formation of stable CV/GqDNA complex as using the measured values of k_+, k_d and k_{-d} as [61],

$$k_r = \frac{k_+ \times k_{-d}}{k_d - k_+} \tag{10}$$

Similarly, we obtain the values of k_{-r} from Eq. (11) using the experimentally measured K, k_d, k_{-d} and k_r above as,

$$K = K_{enc} \times K_{reac} = \frac{k_d}{k_{-d}} \times \frac{k_r}{k_{-r}} \Rightarrow k_{-r} = \frac{k_d}{k_{-d}} \times \frac{k_r}{K} \tag{11}$$

All these measured rate constants are included in Table 3 and Fig. 5. These rate constants clearly indicate that ligand/GqDNA complex formation proceeds on a rugged and complicated free-energy surface. The main observation from Table 3 and Fig. 5 is that the overall association rate constants (k_+) of the ligand binding to GqDNA in the presence of crowders are critically controlled by the diffusion controlled rates, k_d, k_{-d} and k_r, while the ligand unbinding rates (k_{-r}) from the stable complex (the rate-determining step) are nearly unchanged (within error limit) in all crowder solutions. We observe that both the diffusion controlled (collisional) rates, k_d and k_{-d}, are affected by the solution viscosity of crowders. However, the equilibrium constants of encounter complex formation ($K_{enc} = k_d/k_{-d}$) are unchanged for smaller crowders, but decrease nearly to half in the presence of larger (ficoll 70) crowder. This suggests that highly branched ficoll 70 perturbs the solvation shell of GqDNA to a larger extent than the smaller crowders by affecting the local hydration state and/or decreasing the water activity – such that the formation of encounter complex, where the ligand comes within solvation-shell of GqDNA, gets destabilized, leading to lower (collisional) association (k_d) rate and larger dissociation (k_{-d}) rate. These observations are again in line with the above CD spectra and melting data which showed appreciable change by ficoll 70 compared to other two smaller crowders. Because all crowders (smaller or larger) increase the micro-viscosity around GqDNA, the effect of (local) viscosity is also observed on the association rate (k_r) of ligand to G-tetrad which makes the stable ligand/GqDNA complex through π-stacking. We see that all these three rate constants are induced by the local viscosity – leading to

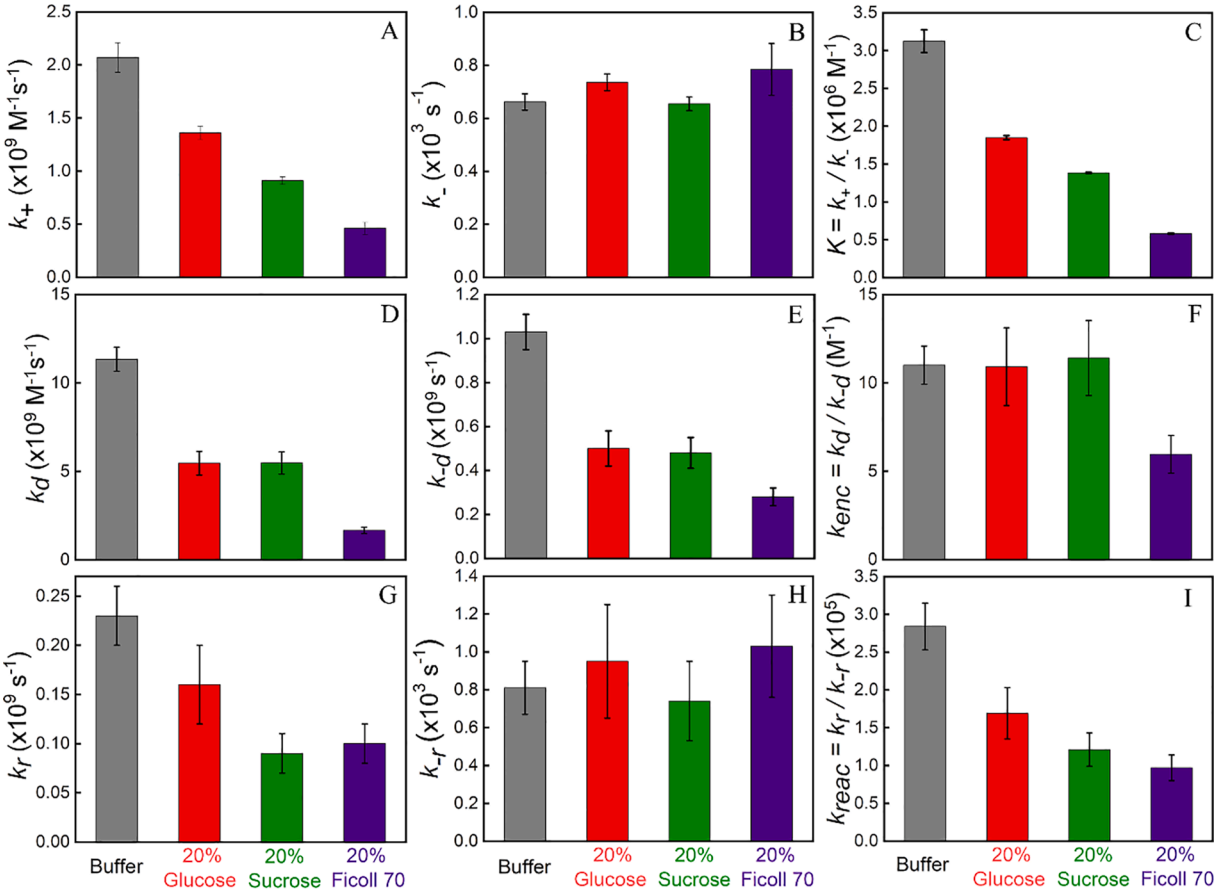

Fig. 5. Bar-graphs showing the relative changes of the kinetic parameters; (A) k_+, (B) k_-, (C) k_+/k_-, (D) k_d, (E) k_{-d}, (F) K_{enc}, (G) k_r, (H) k_{-r}, (I) K_{reac} obtained from the FCS measurements. Data show that the diffusion controlled association rates are the dominating factors which are modulated by the crowder-induced viscosity change. The dissociation rates of the ligand from the stable complex remain nearly unchanged in the presence of the crowders.

the decrease in the overall association rate constants (k_+) of the ligand to GqDNA in the presence of the crowders. However, none of the crowders affect the dissociation (k_{-r}) of the stable ligand/GqDNA complex – leading to nearly unchanged overall dissociation rates (k_-) of ligand from GqDNA in all cases. Thus, it is clear that the chemical properties and/or size of the (saccharide) crowders do not module the π-π interaction between the ligand and the G-tetrad. Because of such large change in k_r and nearly unchanged k_{-r} we observe that the equilibrium constants ($K_{reac} = k_r/k_{-r}$) of the formation of final stable complex decreases with crowder size and solution (micro) viscosity.

The viscosity-induced deceleration of association of two proteins as well as of ssDNA/protein systems in crowded environment have been found in recent studies [37,39]. Using a series of EG and PEG crowders of different sizes and concentrations in a smFRET study on protein/protein interactions, Schuler and co-workers found viscosity-induced deceleration of the association of two proteins at crowder concentrations beyond ~100 mg/ml (10 % w/v), both for smaller or larger crowders [39]. They however, also saw depletion-induced acceleration of the proteins' association in the lower crowder concentrations, with significant effect produced by the larger-sized PEG crowders [39]. Our study however, explores further to obtain all the important individual rate constants which define the overall association and dissociation rates – as to provide a deeper mechanistic details of the ligand/GqDNA interaction. At the crowder concentration used here (20 % w/v) we only observed the viscosity-induced deceleration of ligand association to GqDNA, which is similar to the case of interactions of two (large) intrinsically disordered proteins in crowded conditions found by Schuler and co-workers [39]. However, we note that further studies on same ligand/GqDNA system with varying crowder concentrations are required to check if there is any depletion-induced acceleration of ligand association to GqDNA. A similar crowder induced deceleration of association of ssDNA with protein was observed by Kovermann and co-workers, although they also saw modulation of dissociation rates induced by the crowders which are related to the chemical nature of the crowders [37]. Here, we do not observe such modulation of the dissociation rate of ligand from GqDNA in the presence of crowders. These facts may suggest that though crowders affect the soft electrostatic interactions, including hydrogen-bonding, between DNA and proteins [37], they cannot affect the strong binding interaction of a ligand with G-tetrad of GqDNA which form a stable complex through strong π-π stacking interaction. A cartoon depicting the ligand diffusion, followed by the ligand associations with GqDNA which control the overall association rate, is reproduced in Fig. 6.

3. Conclusion

Even though it was envisaged earlier that molecular crowders affect the binding affinity of ligands to GqDNA structures and the stability of ligand/GqDNA complex, it was unknown how molecular crowding affects the ligand binding *kinetics* with GqDNA. This contribution made a detailed and quantitative investigation of the binding/unbinding interaction kinetics of a benzophenoxazine ligand (CV) with human telomeric GqDNA structure in the presence of (saccharides) crowders of different sizes (molecular weights) at physiological (crowder) concentration. Here we successfully implemented a modified FCS setup to monitor the kinetic steps and measured all the important rate constants of the ligand's interaction with the GqDNA in the absence and presence of crowding agents at (near) single molecule level. We showed that ligand binding affinity to GqDNA is modulated by the crowders which decelerate the association of ligand to GqDNA, primarily induced by the (micro) viscosity change of the solution; however, the dissociation rates remain nearly constant across different samples, which is the main rate-determining step of the overall kinetic process. These results are unique and have important implications in the context of ligand/GqDNA interactions within the cellular environment. The choice of crowders were also made based on the fact that they show marginal impact on the structure and stability of GqDNA, as well as they provide similar volume exclusion in solution – such that we could measure the exclusive effects of (micro) viscosity and crowder size on the ligand binding kinetics with GqDNA. Nevertheless, many more experimental and molecular dynamics simulation studies using enhanced sampling methods are required on these ligand/DNA/crowder systems to comprehend the intricate ligand binding *kinetics* with various nucleic acid structures within cellular environment, and we believe our current study provides the important starting steps to be followed for such future explorations.

CRediT authorship contribution statement

Ndege Simisi Clovis: Methodology, Investigation, Formal analysis, Data curation, Visualization, Validation, Writing – original draft, Writing – review & editing. **Parvez Alam:** Visualization, Validation, Methodology, Investigation, Formal analysis, Data curation, Writing - original draft, Writing - review & editing. **Ajay Kumar Chand:** Visualization, Validation, Methodology, Formal analysis, Data curation, Writing – review & editing. **Deepika Sardana:** Visualization, Validation, Methodology, Formal analysis, Data curation, Writing – review & editing. **Mohammad Firoz Khan:** Methodology, Formal analysis, Data

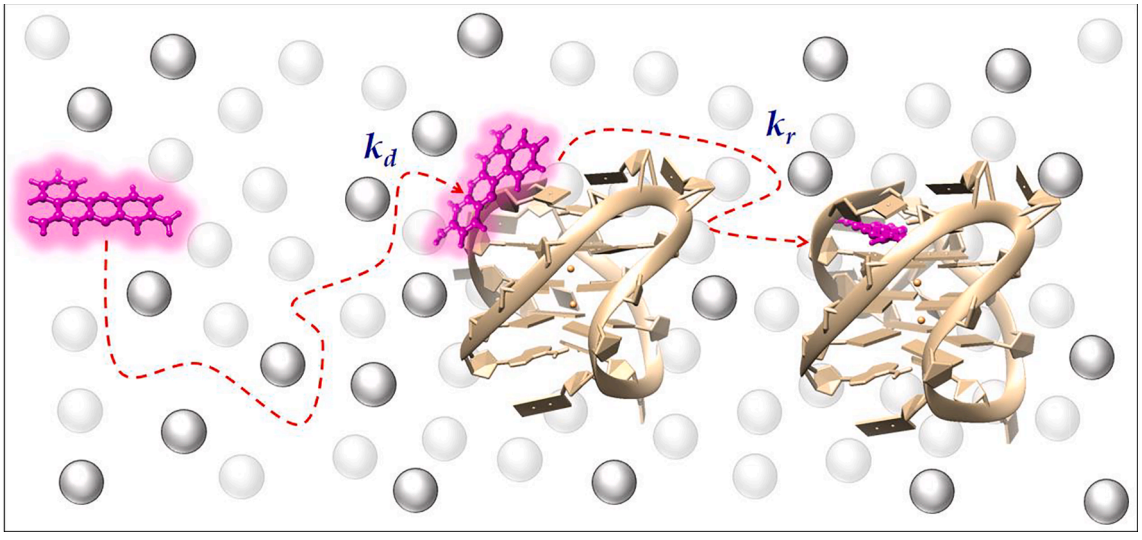

Fig. 6. Cartoon showing the diffusion controlled association which forms the (intermediate) encounter complex where the ligand comes within the solvation shell of GqDNA, followed by the association of ligand into the π-stacked binding-mode with the G-tetrad of GqDNA.

curation, Conceptualization. **Sobhan Sen:** Validation, Supervision, Project administration, Investigation, Funding acquisition, Conceptualization, Data curation, Methodology, Resources, Writing - review & editing.

Declaration of Competing Interest

The authors declare that they have no known competing financial interests or personal relationships that could have appeared to influence the work reported in this paper.

Data availability

Data will be made available on request.

Acknowledgements

This work is supported by Science and Engineering Research Board (SERB), India project granted to S.S. (CRG/2018/002238). CD data were measured at Advanced Instrumentation Research Facility (AIRF), JNU. P.A. thanks UGC; A.K.C. thanks JNU; D.S. and M.F.K. thank CSIR for fellowships.

Appendix A. Supplementary data

Supplementary data to this article can be found online at https://doi.org/10.1016/j.jphotochem.2022.114432.

References

[1] J. Spiegel, S. Adhikari, S. Balasubramanian, The Structure and Function of DNA G-Quadruplexes, Trends Chem. 2 (2) (2020) 123–136.
[2] S. Neidle, G.N. Parkinson, The Structure of Telomeric DNA, Curr. Opin. Struct. Biol. 13 (3) (2003) 275–283.
[3] W.I. Sundquist, A. Klug, Telomeric DNA Dimerizes by Formation of Guanine Tetrads between Hairpin Loops, Nature 342 (6251) (1989) 825–829.
[4] A.T. Phan, V. Kuryavyi, S. Burge, S. Neidle, D.J. Patel, Structure of an Unprecedented G-Quadruplex Scaffold in the Human c-Kit Promoter, J. Am. Chem. Soc. 129 (14) (2007) 4386–4392.
[5] M.L. Zhang, Yeast Telomerase Subunit Est1p has Guanine Guadruplex-Promoting Activity that is Required for Telomere Elongation, Nat. Struct. Mol. Biol. 17 (2010) 202–209.
[6] M.J. McEachern, A. Krauskopf, E.H. Blackburn, Telomeres and their Control, Ann. Rev. Gene. 34 (1) (2000) 331–358.
[7] T. Tian, Y.Q. Chen, S.R. Wang, X. Zhou, G-Quadruplex: A Regulator of Gene Expression and its Chemical Targeting, Chem 4 (2018) 1314–1344.
[8] N. Maizels, L.T. Gray, S.M. Rosenberg, The G4 Genome, PLoS Genet. 9 (4) (2013) e1003468.
[9] A.P. David, E. Margarit, P. Domizi, C. Banchio, P. Armas, N.B. Calcaterra, G-quadruplexes as Novel cis-Elements Controlling Transcription during Embryonic Development, Nucl. Acids Res. 44 (9) (2016) 4163–4173.
[10] R. Simone, P. Fratta, S. Neidle, G.N. Parkinson, A.M. Isaacs, G-quadruplexes: Emerging Roles in Neurodegenerative Diseases and the Non-Coding Transcriptome, FEBS Lett. 589 (2015) 1653–1668.
[11] L. Savva, S.N. Georgiades, Recent Developments in Small-Molecule Ligands of Medicinal Relevance for Harnessing the Anticancer Potential of G-Quadruplexes, Molecules 26 (2021) 841–867.
[12] T. Santos, G.F. Salgado, E.J. Cabrita, C. Cruz, G-Quadruplexes and Their Ligands: Biophysical Methods to Unravel G-Quadruplex/Ligand Interactions, Pharmaceuticals 14 (2021) 769.
[13] S. Asamitsu, S. Obata, Z. Yu, T. Bando, H. Sugiyama, Recent Progress of Targeted G-Quadruplex-preferred Ligands toward Cancer Therapy, Molecules 24 (2019) 429.
[14] A.A. Ahmed, R. Angell, S. Oxenford, J. Worthington, N. Williams, N. Barton, T. G. Fowler, D.E. O'Flynn, M. Sunose, M. McConville, T. Vo, W.D. Wilson, S. A. Karim, J.P. Morton, S. Neidle, Asymmetrically Substituted Quadruplex-Binding Naphthalene Diimide Showing Potent Activity in Pancreatic Cancer Models, ACS Med. Chem. Lett. 11 (8) (2020) 1634–1644.
[15] C. Marchetti, K.G. Zyner, S.A. Ohnmacht, M. Robson, S.M. Haider, J.P. Morton, G. Marsico, T. Vo, S. Laughlin-Toth, A.A. Ahmed, G. Di Vita, I. Pazitna, M. Gunaratnam, R.J. Besser, A.C.G. Andrade, S. Diocou, J.A. Pike, D. Tannahill, R. B. Pedley, T.R.J. Evans, W.D. Wilson, S. Balasubramanian, S. Neidle, Targeting Multiple Effector Pathways in Pancreatic Ductal Adenocarcinoma with a G-Quadruplex-Binding Small Molecule, J. Med. Chem. 61 (6) (2018) 2500–2517.
[16] H. Xu, M.D. Antonio, S. McKinney, V. Mathew, B. Ho, N.J. O'Neil, N.D. Santos, J. Silvester, V. Wei, J. Garcia, F. Kabeer, D. Lai, P. Soriano, J. Banáth, D.S. Chiu, D. Yap, D.D. Le, F.B. Ye, A. Zhang, K. Thu, J. Soong, S.-C. Lin, A.H.C. Tsai, T. Osako, T. Algara, D.N. Saunders, J. Wong, J. Xian, M.B. Bally, J.D. Brenton, G. W. Brown, S.P. Shah, D. Cescon, T.W. Mak, C. Caldas, P.C. Stirling, P. Hieter, S. Balasubramanian, S. Aparicio, CX-5461 is a DNA G-Quadruplex Stabilizer with Selective Lethality in BRCA1/2 Defeicient Tumours, Nat. Commun. 8 (2017) 14432.
[17] K.I.E. McLuckie, Z.A.E. Waller, D.A. Sanders, D. Alves, R. Rodriguez, J. Dash, G. J. McKenzie, A.R. Venkitaraman, S. Balasubramanian, G-Quadruplex-Binding Benzo[a]phenoxazines Down-Regulate c-KIT Expression in Human Gastric Carcinoma Cells, J. Am. Chem. Soc. 133 (2011) 2658–2663.
[18] https://www.g4ldb.com/.
[19] N.S. Clovis, S. Sen, G-Tetrad-Selective Ligand Binding Kinetics in G-Quadruplex DNA Probed with Fluorescence Correlation Spectroscopy, J. Phys. Chem. B 126 (32) (2022) 6007–6015.
[20] S.D. Verma, N. Pal, M.K. Singh, H. Shweta, M.F. Khan, S. Sen, Understanding Ligand Interaction with Different Structures of G-Quadruplex DNA: Evidence of Kinetically Controlled Ligand Binding and Binding-Mode Assisted Quadruplex Structure Alteration, Anal. Chem. 84 (2012) 7218–7226.
[21] S. Paul, S.S. Hossain, B.D. M, A. Samanta, Interactions between a Bioflavonoid and c-MYC Promoter G-Quadruplex DNA: Ensemble and Single-molecule Investigations, J. Phys. Chem. B 123 (2019) 2022−2031.
[22] S.B. Zimmerman, A.P. Minton, Macromolecular Crowding: Biochemical, Biophysical, and Bhysiological Consequences, Annu. Rev. Biophys. Biomol. Struct. 22 (1993) 27–65.
[23] S.-I. Nakano, D. Miyoshi, N. Sugimoto, Effects of Molecular Crowding on the Structures, Interactions, and Functions of Nucleic Acids, Chem. Rev. 114 (5) (2014) 2733–2758.
[24] S.B. Zimmerman, Macromolecular Crowding: Biochemical, Biophysical, and Physiological Consequences, Annu. Rev. Biophys. Biomol. Struct. 22 (1993) 27–65.
[25] R.J. Ellis, Macromolecular Crowding: An Important but Neglected Aspect of the Intracellular Environment, Curr. Opin. Struct. Biol. 11 (2001) 114–119.
[26] S. Takahashi, N. Sugimoto, Stability Prediction of Canonical and Non-Canonical Structures of Nucleic Acids in Various Molecular Environments and Cells, Chem. Soc. Rev. 49 (23) (2020) 8439–8468.
[27] M.C. Miller, R. Buscaglia, J.B. Chaires, A.N. Lane, J.O. Trent, Hydration is a Major Determinant of the G-Quadruplex Stability and Conformation of the Human Telomere 3' Sequence of $d(AG_3(TTAG_3)_3)$, J. Am. Chem. Soc. 132 (48) (2010) 17105–17107.
[28] B. Heddi, A.T. Phan, Structure of Human Telomeric DNA in Crowded Solution, J. Am. Chem. Soc. 133 (25) (2011) 9824–9833.
[29] A. Arora, C. Balasubramanian, N. Kumar, S. Agrawal, R.P. Ojha, S. Maiti, Binding of Berberine to Human Telomeric Quadruplex-Spectroscopic, Calorimetric and Molecular Modeling Studies, FEBS J. 275 (275) (2008) 3971–3983.
[30] Z. Chen, K.-W. Zheng, Y.-H. Hao, Z. Tan, Reduced or Diminished Stabilization of the Telomere G-Quadruplex and Inhibition of Telomerase by Small Chemical Ligands under Molecular Crowding Condition, J. Am. Chem. Soc. 131 (30) (2009) 10430–10438.
[31] H. Rastogi, P.K. Chowdhury, Correlating Local and Global Dynamics of an Enzyme in the Crowded milieu, J. Phys. Chem B 126 (2022) 3208–3223.
[32] H. Rastogi, P.K. Chowdhury, Understanding Enzyme Behavior in a Crowded Scenario through Modulation in Activity, Conformation and Dynamics, BBA-Proteins Proteomics 1869 (2021), 140699.
[33] N. Das, P. Sen, Macromolecular Crowding: How Shape and Interaction affect the Structure, Function, Conformational Dynamics and Relative Domain Movement of a Multi-domain Protein, Phys. Chem. Chem. Phys. 24 (2022) 14242–14256.
[34] N. Das, P. Sen, Shape-Dependent Macromolecular Crowding on the Thermodynamics and Microsecond Conformational Dynamics of Protein Unfolding Revealed at the Single-Molecule Level, J. Phys. Chem. B 124 (28) (2020) 5858–5871.
[35] S. Mukherjee, M.M. Waegele, P. Chowdhury, L. Guo, F. Gai, Effect of Macromolecular Crowding on Protein Folding Dynamics at the Secondary Structure level, J. Mol. Biol. 393 (1) (2009) 227–236.
[36] S.Y. Chung, E. Lerner, Y. Jin, S. Kim, Y. Alhadid, L.W. Grimaud, I.X. Zhang, C. M. Knobler, W.M. Gelbart, S. Weiss, The effect of Macromolecular Crowding on Single-round Transcription by Escherichia coli RNA Polymerase, Nucl. Acids Res. 47 (2019) 1440–1450.
[37] B. Köhn, P. Schwarz, P. Wittung-Stafshede, M. Kovermann, Impact of Crowded Environments on Binding between Protein and Single-stranded DNA, Sci. Rep. 11 (2021) 17682.
[38] P. Dey, A. Bhattacherjee, Role of Macromolecular Crowding on the Intracellular Diffusion of DNA Binding Proteins, Sci. Rep. 8 (2018) 844.
[39] F. Zosel, A. Soranno, K.J. Buholzer, D. Nettels, B. Schuler, Depletion Interactions Modulate the Binding between Disordered Proteins in Crowded Environments, PNAS 117 (24) (2020) 13480–13489.
[40] R. Hänsel, F. Löhr, S. Foldynová-Trantírková, E. Bamberg, L. Trantírek, V. Dötsch, The Parallel G-quadruplex Structure of Vertebrate Telomeric Repeat Sequences is not the Preferred Folding Topology under Physiological Conditions, Nucl. Acids Res. 39 (2011) 5768–5775.
[41] K. Yadav, D. Sardana, H. Shweta, N.S. Clovis, S. Sen, Molecular Picture of the Effect of Cosolvent Crowding on Ligand Binding and Dispersed Solvation Dynamics in G-Quadruplex DNA, J. Phys. Chem. B 126 (8) (2022) 1668–1681.
[42] E. Prado, L. Bonnat, H. Bonnet, T. Lavergne, A. Van der Heyden, G. Pratviel, J. Dejeu, E. Defrancq, Influence of the SPR Experimental Conditions on the G-Quadruplex DNA Recognition by Porphyrin Derivatives, Langmuir 34 (2018) 13057–13064.
[43] A. Christiansen, Q. Wang, A. Samiotakis, M.S. Cheung, P. Wittung-Stafshede, Factors Defining Effects of Macromolecular Crowding on Protein Stability: An in

Vitro/in Silico Case Study Using Cytochrome c, Biochemistry 49 (2010) 6519–6530.
[44] A. Ali, P. Bidhuri, N.A. Malik, S. Uzair, Density, Viscosity, and Refractive Index of Mono-, Di-, and Tri-Saccharides in Aqueous Glycine Solutions at Different Temperatures, Arab. J. Chem. 12 (7) (2019) 1684–1694.
[45] R.B.M. Schasfoort, Introduction to Surface Plasmon Resonance, Handbook of Surface Plasmon Resonance: Edition 2, The Royal Society of Chemistry, UK, 2017.
[46] D. Magde, E. Elson, W.W. Webb, Thermodynamic Fluctuations in a Reacting System-Measurement by Fluorescence Correlation Spectroscopy, Phys. Rev. Lett. 29 (1972) 705–708.
[47] R. Rigler, U. Mets, J. Widengren, P. Kask, Fluorescence Correlation Spectroscopy with High Count Rate and Low Background: Analysis of Translational Diffusion, Eur. Biophys. J. 22 (1993) 169–175.
[48] S. Maiti, U. Haupts, W.W. Webb, Fluorescence Correlation Spectroscopy: Diagnostics for Sparse Molecules, PNAS 94 (1997) 11753–11757.
[49] M. Debnath, S. Ghosh, D. Panda, I. Bessi, H. Schwalbe, K. Bhattacharyya, J. Dash, Small Molecule Regulated Dynamic Structural Changes of Human G-Quadruplexe, Chem. Sci. 7 (2016) 3279–3285.
[50] K. Kawai, E. Matsutani, A. Maruyama, T. Majima, Probing the Charge-Transfer Dynamics in DNA at the Single-Molecule Level, J. Am. Chem. Soc. 133 (39) (2011) 15568–15577.
[51] J. Choi, S. Kim, T. Tachikawa, M. Fujitsuka, T. Majima, pH-induced Intramolecular Folding Dynamics of i-motif DNA, J. Am. Chem. Soc. 133 (40) (2011) 16146–16153.
[52] Y. Yin, L. Yang, G. Zheng, C. Gu, C. Yi, C. He, Y.Q. Gao, X.S. Zhao, Dynamics of Spontaneous Flipping of a Mismatched Base in DNA Duplex, PNAS 111 (22) (2014) 8043–8048.
[53] R. Yadav, B. Sengupta, P. Sen, Conformational Fluctuation Dynamics of Domain I of Human Serum Albumin in the course of Chemically and Thermally Induced Unfolding using Fluorescence Correlation Spectroscopy, J. Phys. Chem. B 118 (2014) 5428–5438.
[54] A. Nandy, S. Chakraborty, S. Nandi, K. Bhattacharyya, S. Mukherjee, Structure, Activity and Dynamics of Human Serum Albumin in a Crowded Pluronic F127 Hydrogel, J. Phys. Chem. B 123 (16) (2019) 3397–3408.
[55] D.K. Sasmal, T. Mondal, S.S. Mojumdar, A. Choudhury, R. Banerjee, K. Bhattacharyya, An FCS Study of Unfolding and Refolding of CPM-Labeled Human Serum Albumin: Role of Ionic Liquid, J. Phys. Chem. B 115 (2011) 13075–13183.
[56] T. Otosu, K. Ishii, T. Tahara, Microsecond Protein Dynamics Observed at the Single-Molecule Level, Nat. Commun. 6 (2015) 7685.
[57] T. Kistwal, A. Mukhopadhyay, S. Dasgupta, K.P. Sharma, A. Datta, Ultraslow Biological Water-Like Dynamics in Waterless Liquid Protein, J. Phys. Chem. Lett. 13 (19) (2022) 4389–4393.
[58] K. Garai, R. Sureka, S. Maiti, Detecting Amyloid-b Aggregation with Fiber-Based Fluorescence Correlation Spectroscopy, Biophys. J. 92 (2007) L55–L57.
[59] S. Wennmalm, V. Chmyrov, J. Widengren, L. Tjernberg, Highly Sensitive FRET-FCS Detects Amyloid β-peptide Oligomers in Solution at Physiological Concentrations, Anal. Chem. 87 (23) (2015) 11700–11705.
[60] A.P. Vavilala, G.S. Victoria, M.F. Khan, D.T. Haokip, B. Yadav, N. Pal, S.C. Sethi, P. Jain, S.L. Singh, S. Sen, S.S. Komath, Ras Hyper activation Versus Over expression: Lessons from Ras Dynamics in Candida Albicans, Sci. Rep. 8 (2018) 5248.
[61] W. Al-Soufi, B. Reija, M. Novo, S. Felekyan, R. Kühnemuth, C.A.M. Seidel, Fluorescence Correlation Spectroscopy, A Tool to Investigate Supramolecuar Dynamics: Inclusion Complexes of Pyronines with Cyclodextrin, J. Am. Chem. Soc. 127 (2005) 8775–8784.
[62] N. Pal, S.D. Verma, M.K. Singh, S. Sen, Fluorescence Correlation Spectroscopy: An Efficient Tool for Measuring Size, Size-Distribution and Polydispersity of Microemulsion Droplets in Solution, Anal. Chem. 83 (2011) 7736–7744.
[63] M.F. Khan, M.K. Singh, S. Sen, Measuring Size, Size Distribution, and Polydispersity of Water-in-Oil Microemulsion Droplets using Fluorescence Correlation Spectroscopy: Comparison to Dynamic Light Scattering, J. Phys. Chem. B 120 (2016) 1008–1020.
[64] S. Sharma, N. Pal, P. Choudhury, S. Sen, A.K. Ganguli, Understanding Growth Kinetics of Nanorods in Microemulsion: A Combined Fluorescence Correlation Spectroscopy, Dynamic Light Scattering and Electron Microscopy Study, J. Am. Chem. Soc. 134 (2012) 19677–19684.
[65] F. Moraca, J. Amato, F. Ortuso, A. Artese, B. Pagano, E. Novellino, S. Alcaro, M. Parrinello, V. Limongelli, Ligand Binding to telomeric G-quadruplex DNA investigated by funnel-metadynamics simulations, PNAS 144 (2017) E2136–E2145.
[66] J. Kim, S. Doose, H. Neuweiler, M. Sauer, The Initial Step of DNA Hairpin Folding: A Kinetic Analysis using Fluorescence Correlation Spectroscopy, Nucl. Acids Res. 34 (2006) 92516–92927.
[67] H.-C. Yeh, C.M. Puleo, Y.-P. Ho, V.J. Bailey, T.C. Lim, K. Liu, T.-H. Wang, Tunable Blinking Kinetics of Cy5 for Precise DNA Quantification and Single-Nucleotide Difference Detection, Biophys. J. 95 (2008) 729–737.
[68] E.F. Caldin, The Mechanisms of Fast Reactions in Solution, IOS Press, Amsterdam, 2001.